Interstellar Chemistry and the life cycles of stars

https://doi.org/10.1017/S1743921317009784 Published online by Cambridge University Press

Astrochemistry VII – Through the Cosmos
from Galaxies to Planets
Proceedings IAU Symposium No. 332, 2017
M. Cunningham, T. Millar & Y. Aikawa, eds.

doi:10.1017/S1743921317009784

Fire from Ice - Massive Star Birth from Infrared Dark Clouds

Jonathan C. Tan[1,2,3]

[1]Dept. of Space, Earth and Environment, Chalmers University, SE-412 96 Gothenburg, Sweden
[2]Dept. of Astronomy, University of Virginia, Charlottesville, VA 22904, USA
[3]Depts. of Astronomy and Physics, University of Florida, Gainesville, FL 32611, USA
email: jctan.astro@google.com

Abstract. I review massive star formation in our Galaxy, focussing on initial conditions in Infrared Dark Clouds (IRDCs), including the search for massive pre-stellar cores (PSCs), and modeling of later stages of massive protostars, i.e., hot molecular cores (HMCs). I highlight how developments in astrochemistry, coupled with rapidly improving theoretical/computational and observational capabilities are helping to improve our understanding of the complex process of massive star formation.

1. Introduction

Massive stars and their associated star clusters are important throughout astrophysics, yet there remain many open questions about how they form. These include: What is the accretion mechanism of massive star formation? What sets the initial mass function of stars, especially at the highest masses? What is the relation of massive star formation to star cluster formation? How do massive star and star cluster formation vary with galactic environment? The nature of the very first, metal-free, i.e., Population III, stars, often theorized to have been of high-mass, is an enduring open question.

In this short review, I focus on theoretical models and observational studies of local, i.e., Galactic, massive star and star cluster formation, concentrating on developments since the reviews of Tan *et al.* (2014, hereafter T14) and Tan (2016) and offering a somewhat different perspective compared to the review of Motte *et al.* (2017). I emphasize the importance of incorporating astrochemistry into theoretical models that try to predict the physical outcome of the massive star formation process, especially to predict the ionization fraction that couples the mainly neutral gas to magnetic fields. Astrochemistry is also crucial for providing diagnostics needed to test different theoretical models.

Following Williams *et al.* (2000) and T14, we define gas *clumps* as self-gravitating structures that fragment into star clusters, perhaps via a population of self-gravitating pre-stellar *cores* (PSCs). These cores are defined to be structures that collapse to a central, rotationally-supported disk leading to single or small-N multiple star formation. As massive stars tend to form in clusters (e.g., de Wit *et al.* 2005), massive star formation and cluster formation are connected processes that need to be understood together.

The observed range of masses of star-forming clumps, including early stage Infrared Dark Clouds (IRDCs), and young star clusters is from $M \sim 10$ to $\sim 10^6\ M_\odot$ (including the most extreme "super star clusters" seen in some relatively nearby galaxies, such as M82, NGC 1569 and NGC 5253), while mass surface densities, Σ, typically range from ~ 0.03 to $\sim 10\ \mathrm{g\ cm^{-2}}$ (i.e., ~ 200 to $\sim 5 \times 10^4\ M_\odot\ \mathrm{pc^{-2}}$) (T14). Thus, protocluster clumps have radii of ~ 1 to 10 pc and average H nuclei number densities of $n_\mathrm{H} \sim 10^3$ to $\sim 10^6\ \mathrm{cm^{-3}}$, although they may contain higher density substructures, including cores.

2. Theoretical Models of Massive Star Formation

2.1. *Overview of Formation Scenarios*

There is a long-standing debate about the basic formation mechanism of massive stars. Theories range from Core Accretion models (e.g., McLaughlin & Pudritz 1997; McKee & Tan 2003 [hereafter MT03], who presented the Turbulent Core Model [TCM]) that are scaled-up versions of standard low-mass star formation theories (Shu, Adams & Lizano 1987), to Competitive Accretion models at the crowded centers of forming star clusters (Bonnell *et al.* 2001; Wang *et al.* 2010) that do not involve massive starless cores, to Protostellar Collisions (Bonnell *et al.* 1998; Bally & Zinnecker 2005; Moeckel & Clarke 2011). Still, as Core Accretion models are the most conservative and simplest way to treat massive star formation and potentially offer a universal mechanism by which to understand all star formation, we will focus mostly on their predictions and comparison to observations, noting cases where these seem to be a relatively poor description.

2.2. *Initial Conditions of the Turbulent Core Model: Massive Pre-Stellar Cores*

The TCM assumes the initial conditions of massive stars are massive PSCs, approximated as polytropic spheres, that are in quasi virial equilibrium and pressure equilibrium with their surrounding clump environment. This implies that a core of mass M_c in a self-gravitating clump of mass surface density $\Sigma_{\rm cl}$, which sets ambient pressure, has radius

$$R_c \simeq 0.0574 (M_c/60\ M_\odot)^{1/2} (\Sigma_{\rm cl}/1\ {\rm g\ cm^{-2}})^{-1/2}\ {\rm pc}, \tag{2.1}$$

(MT03), i.e., 12,000 AU, for fiducial parameter choices, including index of internal power law density profile, $k_\rho = 1.5$. The core has a mass-averaged 1D velocity dispersion of

$$\sigma_c \simeq 1.09 (\phi_B/2.8)^{-1/2} (M_c/60\ M_\odot)^{1/4} (\Sigma_{\rm cl}/1\ {\rm g\ cm^{-2}})^{1/4}\ {\rm km\ s^{-1}}, \tag{2.2}$$

where $\phi_B = 1.3 + 1.5 m_A^{-2}$ accounts for the effects of B-fields, taking a value of 2.8 in the fiducial case of an Alfvén Mach number, m_A, of unity. However, we note that MT03 approximated the magnetic pressure $B^2/(8\pi)$ as isotropic, which it is not. A random magnetic field has an isotropic pressure of $B^2/(24\pi)$, which would reduce ϕ_B, i.e., in this limit the fiducial value would become about 1.8 (C. McKee, private communication).

Note, these conditions apply to the gas structure at the moment just before protostar formation and little is yet assumed about how the core itself formed. By definition, it will have emerged from the clump gas, perhaps via top-down fragmentation, i.e., a massive starless core condensing out of the ambient clump medium, or via bottom-up growth of a smaller gravitationally bound starless core that gains mass by some combination of accretion from the clump or mergers with other cores (such core merging should not be confused with protostellar mergers). The timescale over which the core forms is also not specified: a range of possibilities from very fast, i.e., $t_{\rm c,form} \sim 1 t_{\rm ff}$, where $t_{\rm ff} = (3\pi/[32G\rho])^{1/2} = 1.4 \times 10^5 (n_{\rm H}/10^5\ {\rm cm^{-3}})^{-1/2}$ yr is the local free-fall time of the core given its mean density ρ or equivalently mean H nuclei number density, $n_{\rm H}$, to very slow, i.e., $t_{\rm c,form} \gtrsim 10 t_{\rm ff}$ may be considered. If core formation is a relatively slow process, i.e., $\gtrsim$ a few $t_{\rm ff}$, then the conditions of quasi virial and pressure equilibrium are more likely to be achieved. Note also that while the boundary of a PSC has a precise theoretical definition, i.e., delimiting the material that is gravitationally bound to the core, observationally it can be very challenging to isolate core material by this criterion, especially since the mass surface densities of the core and the surrounding clump have similar values (MT03). We discuss observational definitions of PSCs in §3.1.

The mass scale of a core may potentially be set by its degree of magnetization. If it forms relatively slowly from a more strongly magnetized state as magnetic flux is

https://doi.org/10.1017/S1743921317009784 Published online by Cambridge University Press

gradually removed from the region via ambipolar (e.g., Mouschovias 1991) or reconnection (Lazarian & Vishniac 1999; Eyink *et al.* 2011) diffusion, then it will be close to the boundary between a sub- and super-critical state, i.e., where the B-field strength is just strong enough to impede collapse. Then the mass of the contracting core is effectively set by the magnetic critical mass (e.g., Bertoldi & McKee 1992)

$$M_{\rm c,B} = 51.8(y/0.5)^{-2}(B_c/200\,\mu{\rm G})^3(n_{\rm H,c}/10^5\ {\rm cm}^{-3})^{-2}\ M_\odot, \tag{2.3}$$

where $y \equiv Z/R$ is the aspect ratio (R being the radius normal to axis of symmetry for an ellipsoidal core; $2Z$ being size of core along this axis) here normalized to a moderate degree of flattening along the field direction, B_c is the average magnetic flux in the core (here normalized to a typical value inferred from observations of molecular clouds at this density, Crutcher *et al.* 2010) and $n_{\rm H,c}$ is the mean density of the core. Kunz & Mouschovias (2009) have argued that the entire PSC mass function (PSCMF) may be set by modest variations in the degree of magnetization of gas within star-forming regions.

Eq. (2.2) implies massive PSCs are expected to have internal turbulent motions much greater than the isothermal sound speed at ~ 10 K, i.e., $c_{\rm th} = 0.19(T/10\ {\rm K})^{1/2}\ {\rm km\,s}^{-1}$. Thus they are likely be supersonically turbulent, which would induce internal substructure. The resulting localized shock heating, i.e., up to ~ 50 K for $\sim 1\ {\rm km\,s}^{-1}$ shock speeds, is expected to have astrochemical effects, e.g., liberation of species from grain ice mantles (CO freeze-out being efficient at $\lesssim 20$K) and reduction in the level of deuteration of key diagnostic species N_2D^+ (Kong *et al.* 2015, hereafter K15, see below). Dissipation of energy in these shocks leads to a reduction in the level of turbulence with decay times of about a few $t_{\rm ff}$ (e.g., McKee & Ostriker 2007), which may be partially offset by gravitational contraction of the core. If diffusion of B-field out of the core occurs more slowly, then one expects an evolution towards a state with a lower degree of turbulence, i.e., smaller values of m_A, and a stronger degree of support from large-scale B-fields.

Deuterated species, such as N_2D^+, are thought to be one of the key observational tracers of PSCs (§3.1). This expectation is based on studies of nearby, relatively low-mass PSCs, such as L1544 (e.g., Caselli & Ceccarelli 2012), with observations of such sources leading to the refinement of astrochemical models that aim to predict the abundance of these diagnostic species. High levels of deuteration arise because in the cold, dense conditions relevant to PSCs, CO molecules are mostly frozen-out onto dust grain ice mantles, which allows the abundance of H_2D^+ to build up via the exothermic reaction of $H_3^+ + {\rm HD} \rightarrow H_2D^+ + {\rm o}{-}H_2$, where we have indicated this applies only for the ortho form of H_2. The para form of H_2 has enough energy to drive the reverse reaction. As the ortho-to-para ratio of H_2 ($\rm OPR^{H2}$) drops, e.g., mediated by either gas phase (e.g., Sipilä *et al.* 2015; K15) or grain surface phase (Bovino *et al.* 2017) reactions, this then leads to significant "deuteration fractions", $D_{\rm frac}$, i.e., abundance ratio to the non-deuterated species, of H_2D^+ and N_2D^+ (the latter formed via $H_2D^+ + N_2 \rightarrow H_2 + N_2D^+$).

The gas-phase astrochemistry associated with this deuteration, i.e., including ortho and para spin states, has been studied in the context of one-zone models by, e.g., Sipilä *et al.* (2010, 2015), Wirström *et al.* (2012) and K15, with the latter presenting an exploration of the parameter space relevant to IRDCs/protoclusters and massive PSCs (i.e., $n_{\rm H} = 10^3$ to $10^7\,{\rm cm}^{-3}$, $T = 10$ to 30 K, cosmic ray ionization rates $\zeta = 10^{-18}$ to $10^{-15}\,{\rm s}^{-1}$, assumed fixed gas-phase heavy element depletion factors (a proxy for CO freeze-out) from $f_D = 1$ (no depletion) to 1000 (i.e., total abundance divided by gas phase abundance is 1000), and initial values of $\rm OPR^{H2}$ from $\sim 10^{-3}$ to 3. Some of the main results of this study were the near-equilibrium values of $D_{\rm frac}^{\rm N_2D^+}$ under given conditions and the timescales needed to reach 90% of these near-equilibrium conditions. For example, for conditions of the fiducial

https://doi.org/10.1017/S1743921317009784 Published online by Cambridge University Press

TCM, i.e., $n_{\rm H} \simeq 10^5$ cm^{-3} and $T = 15$ K (and $\zeta = 2.5 \times 10^{-17}$, $f_D = 10$), K15 found $D_{\rm frac,eq}^{\rm N_2D^+} = 0.181$ and the time to reach within 90% of this value to be $t_{\rm eq,90} = 1.25$ Myr (for initial OPR$^{\rm H2} = 0.1$). The fact that this is almost ten times longer than the local free-fall timescale for this density is the reason why the deuteration process may be a useful "chemical clock" to constrain the dynamics of core formation. However, this does depend on correct modeling of the timescale of conversion of ortho to para H_2 (see Bovino *et al.* 2017), as well as the assumption made for the "initial" value of OPR$^{\rm H2}$. Observational constraints on OPR$^{\rm H2}$ are important for breaking such model degeneracies (§3.1).

K15 also presented a series of chemodynamical models, including evolution of f_D by freeze-out and evolution of $n_{\rm H}$ at rates relative to that of free-fall collapse, i.e., following $dn_{\rm H}/dt = \alpha_{\rm ff} n_{\rm H}/t_{\rm ff}$. Again, since the time to reach high levels of deuteration of N_2D^+ can be significantly longer than a local free-fall time, these models can be used in conjunction with observed values of $D_{\rm frac}^{\rm N_2D^+}$ to constrain $\alpha_{\rm ff}$ (§3.1). Such chemodynamical models can be improved to include core radial structure; see, e.g., Pagani *et al.* (2009) for an example of a simple astrochemical model (no spin-state chemistry or N chemistry) applied to low-mass cores and the more general modeling of Gerner *et al.* (2015). Full 3D numerical (M)HD simulation that is fully coupled to an astrochemical network following deuteration is challenging. For example, Körtgen *et al.* (2017) carried out simulations with a reduced network that focussed on H_2D^+ (N_2D^+ was not modeled). Taking an intermediate approach, Goodson *et al.* (2016) analyzed the K15 models to derive analytic expressions for the growth rate of N_2H^+ and N_2D^+ abundances as a function of local density and starting OPR$^{\rm H2}$. These expressions were incorporated in look-up tables to estimate abundances of these species in MHD simulations of massive cores (Fig. 1). These results can be compared to observed candidate massive PSCs (§3.1).

In addition to PSC diagnostics, astrochemical modeling is also needed to estimate ionization fractions in these clouds. For example, for the fiducial parameters of the K15 gas phase astrochemical modeling described above, in particular with $n_{\rm H} = 10^5\,{\rm cm}^{-3}$ and $\zeta = 2.5 \times 10^{-17}\,{\rm s}^{-1}$, $n_e/n_{\rm H}$ is found to range from $\sim 10^{-8}$ when $f_D = 1$ (no depletion) up to $\sim 5 \times 10^{-8}$ in the limit of high f_D. In the case of $f_D = 10$, the positive charge carriers are dominated by about equal fractions of H_3^+ and HCO^+. The ambipolar diffusion time, $t_{\rm ad} = 2.5 \times 10^{13} (n_e/n_{\rm H})$ yr, then has a fiducial value of 5×10^5 yr, i.e., about three times greater than $t_{\rm ff}$. As discussed below, the ionization fraction also depends on assumptions about the dust grain size distribution, which introduces further uncertainties.

2.3. *Massive Protostellar Cores*

In Core Accretion models, a very low-mass ($\ll 1\,M_\odot$) protostar is first expected to form near core center. This acts as a seed for continued accretion from the infall envelope and the structure is now known as a protostellar core. In the fiducial TCM with collapse at rate similar to that of local free-fall, the accretion rate delivered by the infall envelope is

$$\dot{m}_{*d} = 9.3 \times 10^{-4} \epsilon_{*d} (M_c/60\,M_\odot)^{3/4} (\Sigma_{\rm cl}/1\,{\rm g\,cm^{-2}})^{3/4} (M_{*d}/M_c)^{1/2}\,M_\odot\,{\rm yr}^{-1}, \quad (2.4)$$

where $\dot{m}_{*d}$ is the rate of increase of the mass of the protostar and its disk, ϵ_{*d} is the current efficiency of the infall rate with respect to uninhibited collapse (values ~ 0.5 are expected to develope due to protostellar outflow feedback, e.g., Zhang, Tan & Hosokawa 2014 [ZTH14]) and M_{*d} is the idealized collapsed mass supplied to the central disk in the no-feedback limit. Here the ratio M_{*d}/M_c indicates the evolutionary stage of the collapse, i.e., advancing from 0 to 1. The increasing accretion rates during the collapse are a consequence of the assumed initial power law density profile of the PSC of $k_\rho = 1.5$. If an index of 2 is adopted, i.e., that of a singular isothermal sphere, then the accretion rate

https://doi.org/10.1017/S1743921317009784 Published online by Cambridge University Press

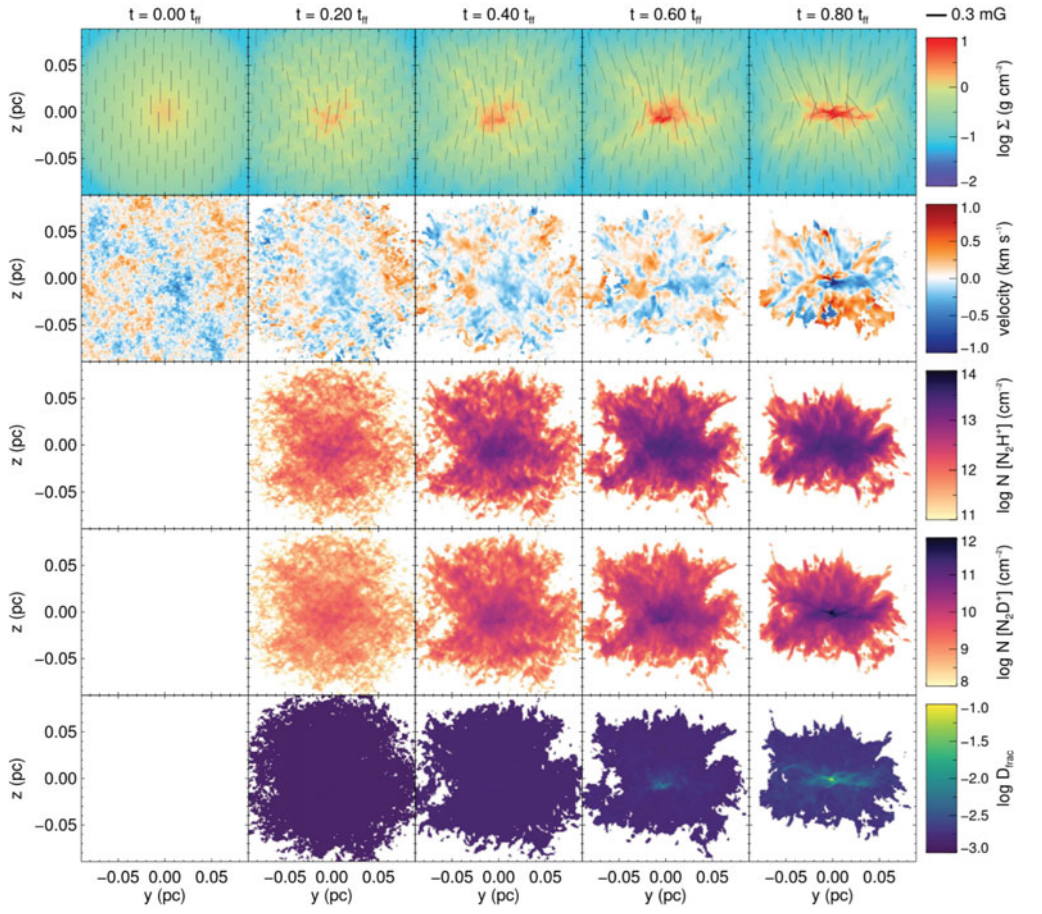

Figure 1. Evolution of a 60 $M_\odot$ PSC embedded in $\Sigma = 0.3$ g cm^{-2} clump (Goodson *et al.* 2016) with properties set by the TCM (MT03). Time evolution is left to right from 0 to 0.8 $t_{\rm ff}$, with initial mean local free-fall time, $t_{\rm ff} = 0.2$ Myr. 1st row: mass surface density, Σ. Total projected B-field strengths and orientations are shown by lines (scale in top right). 2nd row: mean velocity of N_2D^+. 3rd and 4th rows: N_2H^+ and N_2D^+ column densities, via analytic fits to the K15 model. 5th row: $D_{\rm frac}^{\rm N2H+} \equiv [N_2D^+]/[N_2H^+]$. This particular simulated core undergoes relatively fast collapse, so there is little time to build-up very high values of $D_{\rm frac}^{\rm N2H+}$.

would be independent of M_{*d}/M_c. With the fiducial rate of eq. (2.4), the star formation timescale is $t_{*f} = 1.3 \times 10^5 (M_c/60\ M_\odot)^{1/4} (\Sigma_{\rm cl}/1\ {\rm g\,cm^{-2}})^{-3/4}$ yr, which has a weak dependence on M_c. Note, t_{*f} is similar to the clump mean free-fall time, as $t_{*f}/\bar{t}_{\rm ff,cl} \rightarrow 0.98 (M_c/60\ M_\odot)^{1/4} (M_{\rm cl}/4000\ M_\odot)^{-1/4}$. If cluster formation takes many clump free-fall times to complete, then this model allows stars of all masses to form contemporaneously, i.e., with individual formation times that are much shorter than that of the cluster.

Initially protostellar accretion may be quasi spherical, i.e., directly onto the surface of the protostar that is expected to have a radius of several $R_\odot$. Later, as material continues to accrete it is more likely to hit a centrifugal barrier and form an accretion disk, which then mediates accretion and angular momentum transfer, including by launching magneto-centrifugal disk winds and X-winds. For a review of these processes in the context of low-mass star formation, see, e.g., Inutsuka (2012). However, disk formation is a highly uncertain process given the expected role of magnetic braking for transferring angular momentum in the infall envelope (Li *et al.* 2014). Indeed, to fully model this

https://doi.org/10.1017/S1743921317009784 Published online by Cambridge University Press

process appears to require following non-ideal MHD processes, such as ambipolar or reconnection diffusion. To treat ambipolar diffusion requires following the astrochemical evolution to model the small residual ionization fraction in the gas that helps mediate coupling of B-fields to the mostly neutral gas. This requires modeling the propagation of cosmic rays into the central, dense regions of protostellar cores. Zhao *et al.* (2016) have also argued that following the abundance of small dust grains, including PAH molecules, that can act as charge carriers is also needed to make accurate predictions for disk formation. Given the uncertain nature of the initial conditions of massive star formation, e.g., the degree of magnetization of massive PSCs, and given the above complications of following the coupled chemistry and dynamics of the collapse, it is not yet possible to make accurate predictions for the sizes of disks around massive protostars.

The degree of fragmentation in the core will also depend on the magnetization of the PSC. For core formation mediated by magnetic fields, little fragmentation is expected below the magnetic critical mass scale given by eq. (2.3). This expectation is broadly confirmed by the results of numerical simulations. For example, Peters *et al.* (2011) simulated a core with $M_c = 100 M_\odot$, $R_c = 0.5$pc, $n_{\rm H,c} = 5,400 {\rm cm}^{-3}$ and a weak magnetic field of $B_c = 10\,\mu$G. The result of the collapse was a small cluster of protostars. Seifried *et al.* (2011) simulated a core with $M_c = 100\,M_\odot$, $R_c = 0.25$ pc, $n_{\rm H,c} = 4.4 \times 10^4$ cm^{-3} and $B_c \simeq 1$mG, while Myers *et al.* (2013) followed a core with $M_c = 300 M_\odot$, $R_c = 0.1$pc, $n_{\rm H,c} = 2.4 \times 10^6$ cm^{-3} and $B_c \gtrsim 1$ mG. In these latter two simulations no fragmentation was seen, with collapse proceeding approximately monolithically towards a single, central protostar. The effects of radiative heating (e.g., Krumholz *et al.* 2007; Myers *et al.* 2013) further suppress fragmentation, especially during the later, higher-luminosity stages.

Semi-analytic treatments of protostar formation and evolution via the TCM in the limit of no fragmentation have been presented by Zhang & Tan (2011), Zhang, Tan & McKee (2013) and ZTH14. These models include treatments of the slowly rotating infall envelope, a viscous accretion disk, disk wind outflows and protostellar evolution. With the density structure specified by this modeling, the temperature structure is then calculated via Monte Carlo radiative transfer (RT) simulations, including both gas and dust opacities, along with emergent radiation, i.e., to predict multiwavelength images and spectral energy distributions (SEDs). Zhang & Tan (2017) present a suite of such models that cover the parameter space of $M_c = 10$ to $480\,M_\odot$ and $\Sigma_{\rm cl} = 0.1$ to $3\,{\rm g\,cm^{-2}}$. These models have been applied to observed sources by De Buizer *et al.* (2017) (§3.2).

The above models predict that the massive protostar will reach a H-burning phase while still accreting. The photosphere will have a high temperature and be a strong source of FUV and EUV radiation, creating photodissociation regions (PDRs) and HII regions, respectively. Ionizing feedback will first interact with the protostellar outflow, creating an "outflow-confined" HII region that will appear as elongated cm continuum emission (Tan & McKee 2003; Tanaka *et al.* 2016). A combination of radiative and mechanical (outflow) feedback is expected to eventually set the star formation efficiency from the core, ϵ_c. For $M_c = 60\,M_\odot$ and $\Sigma_{\rm cl} = 1\,{\rm g\,cm^{-2}}$, the models of Tanaka *et al.* (2017) have $\epsilon_c \simeq 0.4$. They also find ϵ_c decreases for larger M_c, as feedback from more massive stars is more powerful, and decreases as $\Sigma_{\rm cl}$ decreases, since lower density cores, which have lower accretion rates, are more easily disrupted. Axisymmetric, 2D numerical simulations of mechanical and radiative feedback from massive protostars have been presented by Kuiper *et al.* (2015, 2016) (see also the 3D radiative feedback only simulations of, e.g., Rosen *et al.* 2016 and Harries *et al.* 2017). One key property that is predicted by the above models and simulations is the opening angle of the outflow cavity at a given stage of the protostellar evolution, since this can be compared directly with observed systems.

https://doi.org/10.1017/S1743921317009784 Published online by Cambridge University Press

The modeling of the astrochemistry of the "hot molecular cores" (HMCs) of high-mass protostars has been carried out by a number of groups (e.g., Charnley *et al.* 1992; Caselli *et al.* 1993; Viti *et al.* 2004; Doty *et al.* 2006; Garrod & Herbst 2006; Aikawa *et al.* 2012; Öberg *et al.* 2013; Gerner *et al.* 2014, 2015). Such modeling, typically done as post processing of a given physical model, requires specifying initial chemical conditions, e.g., of the PSC just before star formation, and then the evolution of densities and temperatures along streamlines.

Figure 2, from Drozdovskaya *et al.* (in prep.), shows an example of such modeling for a fiducial massive protostellar infall envelope of the TCM (ZTH14), utilizing a gas-grain network with ∼700 species and 9,000 reactions, including surface chemistry and complex organic species (Drozdovskaya *et al.* 2014, 2015). After a static PSC phase of 3×10^5 yr, the streamlines of the infall envelope are followed for 8.2×10^4 yr, i.e., the time needed to form a 16 $M_\odot$ protostar. The protostar heats the infall envelope, driving astrochemical reactions in the gas and on grain surfaces, and liberating ice species. The figure shows examples of H_2CO gas and ice phase abundances, with the gas phase abundance rising strongly inside $\sim 3,000$ AU. Such models, with outputs then coupled to line radiative transfer codes, are important for making predictions that can be tested with sub-mm/mm observations. However, the full problem of coupled dynamical and chemical evolution, including non-ideal MHD effects and the interaction, via shocks, of protostellar outflows with the infalling core, is challenging to model accurately, given the many inherent uncertainties in both physical and chemical aspects.

2.4. *Massive Star Formation in the Context of Star Cluster Formation*

Aspects of star cluster formation have an impact on massive star formation. As with core formation times, similar uncertainty applies for clumps, i.e., their formation time from surrounding (giant) molecular cloud ([G]MC) gas, $t_{\rm cl,form}$, and the timescale to complete star cluster formation, $t_{*\rm cl,form} = (\epsilon/\epsilon_{\rm ff})\bar{t}_{\rm ff,cl}$, where ϵ is the final star formation efficiency and $\epsilon_{\rm ff}$ is the efficiency per free-fall time. Fast cluster formation in $\sim 1\bar{t}_{\rm ff,cl}$ has been proposed by Elmegreen (2000, 2007), Hartmann & Burkhart (2007) and Hartmann *et al.* (2012). Slower, quasi-equilibrium star cluster formation has been proposed by Tan, Krumholz & McKee (2006) and Nakamura & Li (2007, 2014), with turbulence maintained in the clump by protostellar outflows and/or by accretion (Klessen & Hennebelle 2010; Goldbaum *et al.* 2011). Turbulent gas is expected to have a low rate of star formation (Krumholz & McKee 2005; Padoan *et al.* 2011), i.e., $\epsilon_{\rm ff} \sim 0.02$. Such estimates are consistent with observed protoclusters (e.g., Krumholz & Tan 2007; Krumholz *et al.* 2012; Da Rio *et al.* 2014). Since ϵ needs to be $\gtrsim 0.3$ to form bound star clusters, then, at least in such systems, these estimates of $\epsilon_{\rm ff}$ imply $t_{*\rm cl,form} \sim 10\bar{t}_{\rm ff,cl}$.

The observational search for massive PSCs in protocluster clumps is described in §3.1, however, several points can be considered here to help guide expectations. First, since massive stars are rare, massive PSCs will also be rare objects. Most mass in a clump will not be part of a massive PSC. If we define massive PSCs as having $\gtrsim 16\ M_\odot$, i.e., able to form $\gtrsim 8\ M_\odot$ stars and if the PSCMF is described by a Salpeter (1955) power law of form $dN/d\log M_c \propto M_c^{-\alpha}$ with $\alpha = 1.35$ with lower limit of $M_c = 0.2$ or $1\ M_\odot$ (so that resulting stellar IMFs approximately bracket the characteristics of the observed IMF) and upper limit of $240\ M_\odot$, then the fraction of mass that is in massive cores is 0.144 or 0.272, respectively. Thus a typical mass fraction of cores that can form massive stars is $\simeq 0.2$. If the fraction of the total clump mass that forms PSCs is $\simeq 0.5$, i.e., so that total eventual star formation efficiency is $\simeq 0.25$, then only $\sim 10\%$ of the total clump mass is expected to be processed through massive PSCs. As discussed above, the protostellar phase is expected to take $t_{*f} \simeq 1\bar{t}_{\rm ff,cl}$ and also $t_{*f} \simeq 4.4\bar{t}_{\rm ff,c}$ (MT03). For a

https://doi.org/10.1017/S1743921317009784 Published online by Cambridge University Press

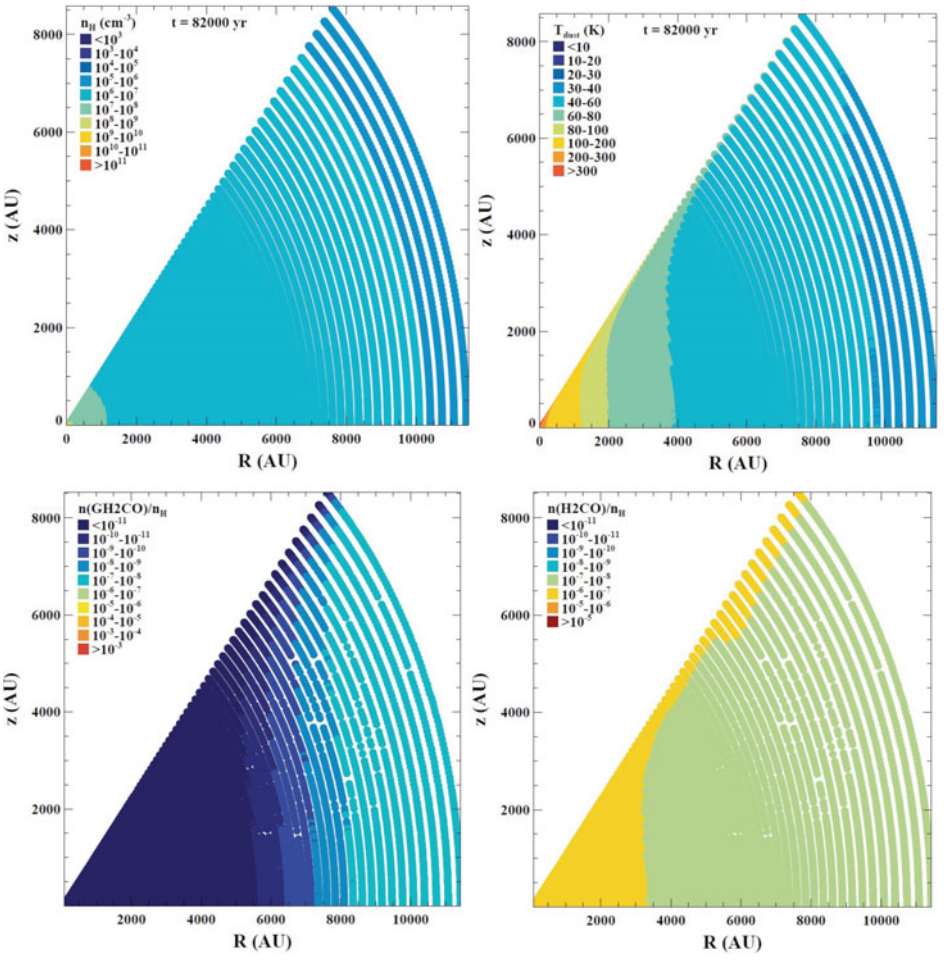

Figure 2. (From Drozdovskaya *et al.*, in prep.; see also Drozdovskaya *et al.* 2017) Astrochemical modeling of the infall envelope of a massive protostar for the case of a 60 $M_\odot$ core embedded in a $\Sigma_{\rm cl} = 1\,{\rm g\,cm^{-2}}$ clump with the protostar now at a mass of 16 $M_\odot$, located in lower left corner of each panel (ZTH14). By this point the outflow cavity has opened up to an angle of $\sim 40^\circ$ (white sector: its density, temperature and chemical structure is not shown here). Note, the accretion disk is also not modeled here. *(a) Top Left:* Density structure ($n_{\rm H}$) at sampling points along streamlines of the infall envelope. *(b) Top right:* Temperature structure. *(c) Bottom Left:* Gas phase abundance of H_2CO relative to $n_{\rm H}$. *(d) Bottom right:* Ice phase abundance of H_2CO relative to $n_{\rm H}$. Note, H_2CO starts evaporating from the grain mantles inside $\sim 7,000$ AU from the protostar and becomes abundant in the gas phase inside $\sim 3,000$ AU.

steady star formation rate and, for simplicity considering closed box models that take $10\bar{t}_{\rm ff,cl}$ to form, then at any given time the observed massive protostellar core population will reflect only 10% of the total that ultimately forms and will only contain 1% of the initial clump mass. Similarly, if the same number of massive PSCs are observed as massive protostellar cores, then this would reflect those PSCs that are within $\simeq 4.4\bar{t}_{\rm ff,c}$ before they form a star (with $\bar{t}_{\rm ff,c}$ defined at this time). The implications of observed PSC and protostellar core demographics are described in §3.1.

Competitive Accretion and Protostellar Collision models both predict that massive protostars will be found near the centers of forming clusters in regions of high (proto)stellar densities. However, Core Accretion models may also predict a preference for massive

https://doi.org/10.1017/S1743921317009784 Published online by Cambridge University Press

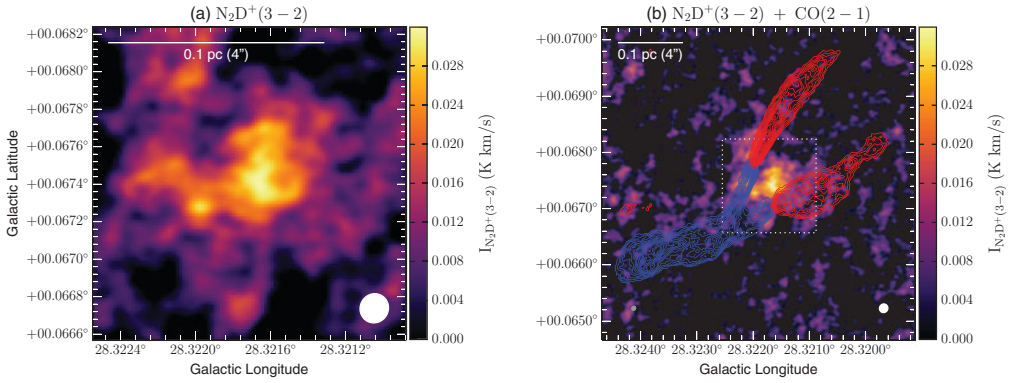

Figure 3. (From Kong *et al.* 2017b) *ALMA* observations of integrated intensity of N_2D^+ (3-2) emission from the G028.37+00.07 (C1-South) massive PSC candidate. The left panel shows a close-up view of the core, with the image smoothed to 0.5 arcsec resolution. The right panel shows an expanded view of the region, now including high velocity CO(2-1) emission revealing two collimated bipolar outflows from nearby, but separate, protostellar sources.

cores to form in denser regions near clump centers, e.g., if massive PSC formation occurs via an agglomeration of smaller PSCs. More isolated massive PSCs are also possible in Core Accretion models. There is a general expectation that massive protostars forming in crowded regions that suffer frequent tidal interactions with nearby stars will have smaller accretion disks and more disturbed accretion geometries. For example, the orientation of the disk and outflows would vary more in Competitive Accretion than Core Accretion models. Strong accretion variability, i.e., bursts, would also be expected to result from these interactions. However, accretion bursts due to disk instabilities and, more slowly, via infall variation in turbulent cores, are also possible in Core Accretion models.

3. Observational Studies of Massive Star Formation

3.1. *The Search for Massive Pre-Stellar Cores*

One of the best studied "low-mass" PSCs is L1544 (Caselli & Ceccarelli 2012). However, this core actually has $\sim 8\,M_\odot$, i.e., is quite massive, and its slow, subsonic infall ($\lesssim$10% of free-fall), suggests B-fields play a significant role in its dynamics (Keto *et al.* 2015).

Searches for more massive PSCs in higher $\Sigma_{\rm cl}$ environments have focussed on IRDCs. Tan *et al.* (2013), following up a sub-sample of the Butler & Tan (2012) MIR extinction map peaks, identified six cores via $N_2D^+(3-2)$ emission. Follow-up observations of the C1-S source identified protostellar outflows in its vicinity (Tan *et al.* 2016), but analysis of the highest resolution, highest sensitivity data (Kong *et al.* 2017b) indicates that C1-S, as defined by its $N_2D^+(3-2)$ emission, is spatially and kinematically distinct from these sources and is thus a promising massive PSC candidate (Fig. 3). The mass estimate, based on mm dust continuum emission, is about $50\,M_\odot$ inside a radius of 0.045 pc, depending on assumed dust temperature (fiducial value of 10 K). This implies a mean density of $n_{\rm H} \simeq 4\times10^6\,{\rm cm}^{-3}$. Note that due to systematically cooler temperatures, PSCs like C1-S do not stand out as strong continuum sources, especially compared to protostellar cores.

The velocity dispersion of C1-S is measured to be 0.28 km/s, which is about 1/3 of the level expected from virial equilibrium of the fiducial TCM core (eq. 2.2). For the core to be in virial equilibrium would require stronger large-scale B-fields, i.e., ~ 3 mG, so that the Alfvén Mach number is about 0.2. Such B-field strengths are similar to those predicted

https://doi.org/10.1017/S1743921317009784 Published online by Cambridge University Press

using the empirical relation $B_{\rm median} \simeq 0.22(n_{\rm H}/10^5\ {\rm cm}^{-3})^{0.65}$ mG (for $n_{\rm H} > 300\,{\rm cm}^{-3}$) (Crutcher *et al.* 2010), to those observed on larger scales in some IRDCs (Pillai *et al.* 2015) and to values inferred in some massive protostars (§3.2).

The deuteration fraction of C1-S was measured by Kong *et al.* (2016) to be $D_{\rm frac}^{\rm N2D+} \sim 0.15$ to 0.7. These values are similar to the equilibrium values of the K15 astrochemical models for the relevant physical conditions of the core. The timescales to reach this level of deuteration are $\gtrsim 10^5$ yr, significantly longer than the $\sim 2\times10^4$ yr free-fall time. Most chemodynamical models require relatively slow collapse compared to free-fall ($\alpha_{\rm ff} \lesssim 0.3$). Conversely, the example simulated core of Goodson *et al.* (2016), which undergoes more rapid collapse (Fig. 1), does not reach such high levels of $D_{\rm frac}^{\rm N2D+}$. Still, rapid collapse models can be made compatible if the starting value of $\rm OPR^{H2}$ is very low (but which itself may then require multiple free-fall times) or if ortho to para H_2 conversion rates are dramatically sped up compared to gas phase estimates (Bovino *et al.* 2017). Observational contraints on $\rm OPR^{H2}$ are needed to help break these degeneracies. Brüncken *et al.* (2014) achieved this for the low-mass protostellar core IRAS 16293-2422 A/B via observations of ortho- and para-H_2D^+, estimating it has a chemical age of >1 Myr, i.e., $> 10t_{\rm ff}$. Similar studies are needed of more massive cores.

To increase the sample size of massive PSCs, Kong *et al.* (2017a) searched 30 IRDC clumps for N_2D^+(3-2) emission. Several promising candidates were detected. Dynamical analysis of the 6 strongest sources was carried out. Together with the 6 cores analyzed by Tan *et al.* (2013), overall this sample of 12 intermediate- and high-mass PSC candidates have observed velocity dispersions that are quite similar, within a factor of ∼0.8, compared to the fiducial virial equilibrium value of eq. (2.2).

Cyganowski *et al.* (2014) reported G11.920.61-MM2 as a massive PSC candidate. However, the non-detection of any molecular lines from this source is peculiar and makes it difficult to assess the reliability of the structure, e.g., via a dynamical mass measurement. The Cygnus X N53 MM2 core (Bontemps *et al.* 2010) and G11P6-SMA1 (Wang *et al.* 2014) are other potential massive PSCs based on the absence of obvious outflows (see also Motte *et al.* 2017). Sanhueza *et al.* (2017) searched IRDC G028.23-00.19 for massive PSCs. Given its current mass of 1,500 $M_\odot$, if it were to form a star cluster of $\sim 500\,M_\odot$, then the median expected mass of the most massive star would be about 26 $M_\odot$ (for Salpeter IMF from 0.1 to 120 $M_\odot$), so a $\sim 50\,M_\odot$ PSC is expected at some stage in the clump. However, Sanhueza *et al.* find five cores with masses up to only $\sim 15\,M_\odot$, though these do appear to be starless, i.e., lacking outflows. Such results may indicate that the most massive core has not yet formed. Note, if cluster formation is slow, then at any instant, only a small fraction $\sim \epsilon_{\rm ff}/\epsilon$ of the core population would be present.

Motte *et al.* (2007) and Russeil *et al.* (2010) (see also Motte *et al.* 2017) estimated massive PSC and starless clump lifetimes as short as $\lesssim 1$ to 3×10^4 yr in Cygnus X and NGC6334/NGC6357, by comparing to numbers of O to B3 stars and assigning a timescale of a few Myr to these stars. In addition to the already mentioned difficulty of identifying PSCs via dust continuum if they are systematically colder than protostellar cores and the ambient clump (e.g., Russeil *et al.* adopt a fiducial temperature of 20 K for their mass estimates), another potential problem with this analysis is that only core/clumps of $\geqslant 40 M_\odot$ and $\geqslant 200 M_\odot$ were counted in Cygnus X and NGC6334/NGC6357, respectively. For example, in the fiducial TCM, PSCs with masses $\sim 16\,M_\odot$ are expected to be able to produce $\sim 8\,M_\odot$ stars, i.e., B3 stars on the zero age main sequence.

3.2. *Massive Protostars, Accretion Disks, Outflows and Hot Molecular Cores*

Csengeri *et al.* (2017) studied mm dust continuum emission from 35 infrared quiet massive clumps, finding many examples of massive, protostellar cores that show limited

https://doi.org/10.1017/S1743921317009784 Published online by Cambridge University Press

fragmentation: most regions are dominated by just one or a few cores. The presence of strong B-fields is a plausible explanation for the limited degree of fragmentation in these sources, rather than, e.g., radiative heating. On the other hand, Cyganowski *et al.* (2017) have argued that there is a relatively high degree of fragmentation present in the G11.92-0.61 region. If massive stars are forming in an unbiased way within protoclusters, then, even in the context of Core Accretion models, one expects that many lower-mass protostellar cores will also be found in their vicinity.

Dynamically strong B-fields in massive protostellar cores have been inferred by Girart *et al.* (2009) and Zhang *et al.* (2014) from mm/sub-mm polarization observations. Vlemmings *et al.* (2010) measured even stronger B-field strengths of ~ 20 mG via 6.7 GHz methanol maser emission within $\sim 1,000$ AU of Cep A HW2.

Infall has been detected in 9 sources by Wyrowski *et al.* (2016), though it can be difficult to tell if this is at the clump or core scale. These authors find slow infall speeds: on average only $\sim 10\%$ of the free-fall speed. Processes that may slow infall include support from B-fields and/or maintenance of clump turbulence by outflows and accretion.

The search for and characterization of rotationally supported disks remains challenging, which is not unexpected if diameters are $\lesssim 1,000$ AU, i.e., $\lesssim 0.5$" at 2 kpc. Since the review of T14, there have been several claims of detection of such disks (e.g., Ilee *et al.* 2016; Beuther *et al.* 2017a), with these studies utilizing emission of CH_3CN. In the latter work, the authors achieve 130 AU resolution, find limited fragmentation on the core scale and conclude the disk itself is also stable with respect to gravitational instability.

Collimated molecular outflows are often a feature of massive protostars (e.g., Beuther *et al.* 2002; Duarte-Cabral *et al.* 2013; see also Fig. 3, where the northern protostellar source is estimated to have a core mass of $\sim 30\,M_\odot$, Kong *et al.* 2017b). On small scales relevant to outflow launching, Hirota *et al.* (2017) have presented a high-resolution study of the closest example of a massive protostar, Orion source I, finding evidence of rotation near the base of the outflow, consistent with disk wind models. During the later stages of formation and for the more massive systems, the outflows are expected to become photoionized by the protostar. Ionized, collimated outflows traced as radio continuum "jets" have been seen in some massive protostars (e.g., Gibb *et al.* 2003; Guzmán *et al.* 2014), although the relative importance of shock- versus photo-ionization remains to be established. Cm continuum emission from ionized gas remains the most promising method to identify the precise locations of massive protostars over a range of evolutionary stages (e.g., Rosero *et al.* 2016), including detecting the presence of multiplicity (e.g., Beuther *et al.* 2017b). A growing sample of massive protostars, such as G35.20-0.74N, now have their IR to mm SEDs well-characterized and fit to predictions of the TCM (Zhang *et al.* 2013b; De Buizer *et al.* 2017). Elongation in the images from 10 to 40 μm is expected along the outflow cavity and this information helps to constrain the RT models. The goal of such studies is to determine to what extent simple, symmetric protostellar models can explain the observed dust continuum and, eventually, spectral line morphologies. The presence of order and symmetry in core and outflow features, especially when maintained over large scales, is not expected in Competitive Accretion and Protostellar Collision models. Core Accretion models may also exhibit spatial asymmetries, e.g., due to low-order multiplicity resulting from disk fragmentation and/or disk axis precession, as well as temporal variability, e.g., due to disk instabilities. Accretion bursts revealed by luminosity variations have been reported by Caratti o Garatti *et al.* (2017) and Hunter *et al.* (2017).

There are some examples of more disordered outflows, with the larger-scale outflow from the Orion KL region, potentially driven by source I, being a prime example (e.g., Bally *et al.* 2017). Dynamical interaction among protostellar and young stellar sources, some of which are now high proper motion runaway stars (e.g., Luhman *et al.* 2017) seems

https://doi.org/10.1017/S1743921317009784 Published online by Cambridge University Press

likely to have played a role in triggering the apparently "explosive" outflow, although the precise details of how this has occurred remain debated (e.g., Bally & Zinnecker 2005; Chatterjee & Tan 2012). It should be noted that the chemical complexity of the Orion Hot Core (e.g., Schilke *et al.* 2001; Crockett *et al.* 2010) is likely to have been affected by the strong shocks resulting from this enhanced outflow activity. Another potential example of an explosive outflow is the DR21 system (Zapata *et al.* 2013), but such systems appear to be relatively rare in the massive protostar population.

4. Summary and Outlook

Massive star formation involves many different complex physical and chemical processes that need to be followed over vast ranges of spatial and temporal scales. The initial conditions of the problem are poorly constrained and often poorly defined. However, there is progress driven by improving theoretical/computational modeling and improving observational capabilities. Astrochemical modeling has crucial roles to play in helping to carry out physical modeling, e.g., of ambipolar diffusion during the collapse of pre- and protostellar cores, and for interpretation of observational signatures of the various evolutionary phases of the massive star formation process. However, given the large uncertainties present in both physical and chemical models, great caution is needed when developing and interpreting model results. Careful testing of predictions against observations to then refine the models is essential.

Acknowledgements

We thank Chris McKee for helpful comments on the manuscript. We thank Maria Drozdovskaya, Matthew Goodson and Shuo Kong for providing figures from their papers.

References

Aikawa Y., Wakelam V. *et al.* 2012, *ApJ*, 760, 40
Bally, J., Ginsburg, A., Arce, H. *et al.* 2017, *ApJ*, 837, 60
Bally, J. & Zinnecker, H. 2005, *AJ*, 129, 2281
Beuther, H., Linz, H., Henning, Th. *et al.* 2017b, *ApJ*, 605, 61
Beuther, H., Schilke P. *et al.* 2002, *A&A*, 383, 892
Beuther, H., Walsh, A. J., Johnston, K. G. *et al.* 2017a, *A&A*, 603, 10
Bonnell, I. A., Bate, M., Clarke, C. J., & Pringle, J. E. 2001, *MNRAS*, 323, 785
Bonnell, I. A., Bate, M., & Zinnecker, H. 1998, *MNRAS*, 298, 93
Bontemps S., Motte F., Csengeri, T. & Schneider N. 2010, *A&A*, 524, 18
Bovino, S., Grassi, T., Schleicher, D. R., & Caselli, P. 2017, arXiv:1708.02046
Brüncken, S., Sipilä, O., Chambers, E. T. *et al.* 2014, *Nature*, 516, 219
Butler M. J. & Tan J. C., 2012, *ApJ*, 754, 5
Caratti o Garatti, A., Stecklum, B., Garcia Lopez, R. *et al.* 2017, *Nature Physics*, 13, 276
Caselli, P. & Ceccarelli, C. 2012, *A&AR*, 20, 56
Caselli P., Hasegawa T. *et al.* 1993, *ApJ*, 408, 548
Charnley S. B. *et al.* 1992, *ApJ*, 399, L71
Chatterjee, S. & Tan, J. C. 2012, *ApJ*, 754, 152
Crockett, N. R., Bergin, E. A., Wang, S. *et al.* 2010, *A&A*, 521, L21
Crutcher, R. M., Wandelt, B., Heiles, C., *et al.* 2010, *ApJ*, 725, 466
Csengeri, T. Bontemps, S., Wyrowski, F. *et al.* 2017, *A&A*, 600, L10
Cyganowski, C. J., Brogan, C. L., Hunter, T. R. *et al.* 2014, *ApJL*, 796, 2
Cyganowski, C. J., Brogan, C. L., Hunter, T. R. *et al.* 2017, *MNRAS*, 468, 3694
Da Rio, N., Tan, J. C., & Jaehnig, K. 2014, *ApJ*, 795, 55
De Buizer, J. M., Liu, M., Tan, J. C. *et al.* 2017, *ApJ*, 843, 33

de Wit, W. J., Testi, L., Palla, F., & Zinnecker, H. 2005, *A&A*, 437, 247
Doty, S. D., van Dishoeck, E. F., & Tan, J. C. 2006, *A&A*, 454, L5
Drozdovskaya, M., Tan, J. C. *et al.* 2017, in *Star Formation from Cores to Clusters*, 19
Drozdovskaya, M., Walsh, C., Visser, R. *et al.* 2014, *MNRAS*, 445, 913
Drozdovskaya, M., Walsh, C., Visser, R. *et al.* 2015, *MNRAS*, 451, 3836
Duarte-Cabral A. *et al.* 2013, *A&A*, 558, 125
Elmegreen, B. G. 2000, *ApJ*, 530, 277
Elmegreen, B. G. 2007, *ApJ*, 668, 1046
Eyink, G. L., Lazarian, A., & Vishniac, E. T. 2011, *ApJ*, 743, 51
Garrod R. T. & Herbst E. 2006 *A&A*, 457, 927
Gerner, T., Beuther, H., Semenov, D. *et al.* 2014, *A&A*, 563, 97
Gerner, T., Shirley, Y. L., Beuther, H. *et al.* 2015, *A&A*, 579, 80
Gibb, A. G. *et al.* 2003, *MNRAS*, 339, 198
Girart, J. M., Beltrán, M. T., Zhang, Q. *et al.* 2009, *Science*, 324, 1408
Goldbaum, N. J., Krumholz, M. R., Matzner, C. D., & McKee, C. F. 2011, *ApJ*, 738, 101
Goodson, M. D., Kong, S., Tan, J. C., Heitsch, F., & Caselli, P. 2016, *ApJ*, 833, 274
Guzmán, A. E., Garay, G., Rodríguez, L. F., *et al.* 2014, *ApJ*, 796, 117
Harries, T. J., Douglas, T. A., & Ali, A. 2017, *MNRAS*, 471, 4111
Hartmann, L., Ballesteros-Paredes, J., & Heitsch, F. 2012, *MNRAS*, 420, 1457
Hartmann, L. & Burkert, A. 2007, *ApJ*, 654, 988
Hirota, T., Machida, M. N., Matsushita, Y. *et al.* 2017, *Nature Astronomy*, 1, 146
Hunter, T. R., Brogan, C. L., MacLeod, G. *et al.* 2017, *ApJ*, 837, L29
Inutsuka, S. 2012, *PTEP*, 2012, 01A307
Keto, E., Caselli, P., & Rawlings, J. 2015, *ApJ*, 446, 3731
Klessen, R. S. & Hennebelle, P. 2010, *A&A*, 520, 17
Körtgen, B. Bovino, S., Schleicher, D. R. G. *et al.* 2017, *MNRAS*, 469, 2602
Kong, S., Caselli, P., Tan, J. C. *et al.* 2015, *ApJ*, 804, 98
Kong, S., Tan, J. C., Caselli, P. *et al.* 2016, *ApJ*, 821, 94
Kong, S., Tan, J. C., Caselli, P. *et al.* 2017a, *ApJ*, 834, 193
Kong, S., Tan, J. C., Caselli, P. *et al.* 2017b, *ApJ*, sub. (arXiv:1701.05953)
Krumholz, M. R., Dekel, A., & McKee, C. F. 2012, *ApJ*, 745, 69
Krumholz, M. R., Klein, R. I. *et al.* 2007, *ApJ*, 656, 959
Krumholz, M. R. & McKee, C. F. 2005, *ApJ*, 630, 250
Krumholz, M. R. & Tan, J. C. 2007, *ApJ*, 654, 304
Kuiper, R., Turner, N. J. & Yorke H. W. 2015, *ApJ*, 800, 86
Kuiper, R., Turner, N. J. & Yorke H. W. 2016, *ApJ*, 832, 40
Kunz, M. W. & Mouschovias, T. Ch. 2009, *MNRAS*, 399, L94
Lazarian, A. & Vishniac, E. T. 1999, *ApJ*, 517, 700
Li, Z.-Y., Banerjee, R., Pudritz, R. E. *et al.* 2014, *PPVI*, eds. Beuther *et al.*, U. Arizona, p173
Luhman, K. L., Robberto, M., Tan, J. C. *et al.* 2017, *ApJ*, 838, L3
McLaughlin, D. E & Pudritz, R. E. 1997, *ApJ*, 476, 750
McKee, C. F. & Ostriker, E. C. 2007, *ARA&A*, 45, 565
McKee, C. F. & Tan, J. C. 2003, *ApJ*, 585, 850 [MT03]
Moeckel, N. & Clarke, C. J. 2011, *MNRAS*, 410, 2799
Motte, F., Bontemps, S., Schilke, P., *et al.* 2007, *A&A*, 476, 1243
Motte, F., Bontemps, S., & Louvet, F. 2017, *AR&A*, in press (arXiv:1706.00118)
Mouschovias, T. Ch. 1991, *ApJ*, 373, 169
Myers A. T., McKee C. F. *et al.* 2013, *ApJ*, 766, 97
Nakamura, F. & Li, Z-Y. 2007, *ApJ*, 662, 395
Nakamura, F. & Li, Z-Y. 2014, *ApJ*, 783, 115
Öberg K. I., Boamah M. *et al.* 2013, *ApJ*, 771, 95
Padoan, P. & Nordlund, A. 2011, *ApJ*, 730, 40
Pagani, L., Vastel, C., Hugo, E., *et al.* 2009, *A&A*, 494, 623
Peters, T., Banerjee, R., Klessen, R. S., & Mac Low, M.-M. 2011, *ApJ*, 729, 72

Pillai, T., Kauffmann, J., Tan, J. C. *et al.* 2015, *ApJ*, 799, 74
Rosen, A., Krumholz, M. R., McKee, C. F., & Klein, R. I. 2016, *MNRAS*, 63, 2553
Rosero, V., Hofner, P., Classen, M. *et al.* 2017, *ApJS*, 227, 25
Russeil D., Zavagno A., Motte F. *et al.* 2010 *A&A*, 515, 55
Salpeter, E. E. 1955, *ApJ*, 121, 161
Sanhueza, P., Jackson, J. M., Zhang, Q. *et al.* 2017, *ApJ*, 841, 97
Schilke, P. Benford, D. J., Hunter, T. R. *et al.* 2001, *ApJS*, 132, 281
Seifried, D., Banerjee, R., Klessen R. S. *et al.* 2011, *MNRAS*, 417, 1054
Sipilä, O., Caselli, P., & Harhu, J. 2015, *A&A*, 578, 55
Sipilä, O., Hugo, E., Harju, J. *et al.* 2010, *A&A*, 509, A98
Shu, F. H., Adams, F. C., & Lizano, S. 1987, *ARA&A*, 25, 23
Tan, J. C. 2016, *From Interstellar Clouds to Star-Forming Galaxies*, IAU Symp., 315, 154
Tan, J. C., Beltrán, M., Caselli, P. *et al.* 2014, *PPVI*, eds. Beuther *et al.*, U. Arizona, p149 [T14]
Tan, J. C., Kong, S., Butler, M. J., Caselli, P., & Fontani, F. 2013, *ApJ*, 779, 96
Tan, J. C., Kong, S. Caselli, P. *et al.* 2016, *ApJ*, 821, L3
Tan, J. C., Krumholz, M. R., & McKee, C. F. 2006, *ApJ*, 641, L121
Tan, J. C. & McKee, C. F. 2003, astro-ph/0309139
Tanaka, K. E. I., Tan, J. C., & Zhang, Y. 2016, *ApJ*, 818, 1
Tanaka, K. E. I., Tan, J. C., & Zhang, Y. 2017, *ApJ*, 835, 32
Viti S. *et al.* 2004, *MNRAS*, 354, 1141
Vlemmings W. *et al.* 2010, *MNRAS*, 404, 134.
Wang, P. Li, Z-Y., Abel, T., & Nakamura, F. 2010, *ApJ*, 709, 27
Wang K., Zhang Q., Testi L. *et al.* 2014, *MNRAS*, 439, 3275
Williams, J. P., Blitz, L., & McKee, C. F. 2000, *PPV*, eds. Mannings *et al.*, U. Arizona, p97
Wirström, E. S., Charnley, S. B., Cordiner, M. A., & Milam, S. N. 2012, *ApJL*, 757, L11
Wyrowski, F., Güsten, R., Menten, K. M. *et al.* 2016, *A&A*, 585, 149
Zapata, L. A., Schmid-Burgk, J., Pérez-Goytia, N. *et al.* 2013, *ApJ*, 765, L29
Zhang, Q., Qiu, K., Girart, J. M. *et al.* 2014, *ApJ*, 792, 116
Zhang, Y. & Tan, J. C. 2011, *ApJ*, 733, 55
Zhang, Y. & Tan, J. C. 2015, *ApJL*, 802, L15
Zhang, Y. & Tan, J. C. 2017, *ApJ*, submitted (arXiv:1708.08853)
Zhang, Y., Tan, J. C., & Hosokawa, T. 2014, *ApJ*, 788, 166 [ZTH14]
Zhang, Y., Tan, J. C., De Buizer *et al.* 2013b, *ApJ*, 767, 58
Zhang, Y., Tan, J. C. & McKee 2013a, *ApJ*, 766, 86
Zhao, B., Caselli, P., Li, Z.-Y. *et al.* 2016, *MNRAS*, 460, 2050